

CYCLOPARAPHENYLENES AND THEIR BIOLOGICAL
APPLICATIONS

by

ANNA GARRISON

A THESIS

Presented to the Department of Biochemistry
and the Robert D. Clark Honors College
in partial fulfillment of the requirements for the degree of
Bachelor of Science

February 2022

An Abstract of the Thesis of

Anna Garrison for the degree of Bachelor of Science
in the Department of Chemistry and Biochemistry to be taken February 2022

Title: Cycloparaphenylenes and their Biological Application

Approved: *Ramesh Jasti, Ph.D.*
Primary Thesis Advisor

Looking inside the human body is a critical tool researchers and physicians need to explore the human species, navigate and discover new diseases, and look for new cures or therapies. It is impossible to visualize and explore its intricate detail without an effective way to mark structures of interest with fluorescent probes. Fluorophores are chemical markers that attach to specific structures and cause them to emit visible light. They function by absorbing a light from some source and re-emit that light at a certain wavelength. It is important there are a wide variety of fluorophores as they each emit a unique wavelength that can be used for a variety of biochemical purposes. The most widely used commercially available fluorophore is the Green Fluorescent Protein (also known as GFP) which has very successfully utilized genetic encoding to embed green fluorescence in targeted molecules. One of the most important limitations with this approach is its inability to fluoresce genetically modified biomolecules.

[*n*]cycloparaphenylenes or “CPPs” are a class of molecules with unique structure that causes a useful size-dependent fluorescence property. This property allows researchers to design various structures with varying colors. The stepwise synthetic nature with which CPPs are created allows them to be easily manipulated to

insert useful chemical structures which alter the electrical and photophysical properties. These unique reactive and optical properties have made CPPs an attractive material studied for the purpose of biological imaging. Previous research has been conducted to investigate the effectiveness of CPPs as biological fluorophores. A CPP that is non-cytotoxic, water-soluble, and capable of permeating cell membranes has been reported. This is the first account that demonstrated CPPs could be suitable for cellular environments.

Macrocyclic angle-strained alkyne CPPs (CPPs with a carbon-carbon triple bond incorporated into their cyclic structure) are a unique class of CPPs that can be used for tagging biological molecules through copper-free click chemistry. Copper-free click chemistry such as the strain-promoted alkyne-azide reaction (also known as the SPAAC reaction) is a unique way to attach two molecules together (ligation reaction) in a living system that avoids the cytotoxicity of copper, a common dangerous chemical. This is a simple and safe reaction that can leave biological systems unharmed. Introducing an alkyne (a carbon-carbon triple bond) into the ring of the CPP boosts the reactivity of the molecule and the ability to click to biomolecules through the SPAAC reaction.

Here we explore the stability of alkyne CPPs in biological environments, demonstrating stability at physiological temperature. We also successfully click an alkyne CPP to a biomolecule. Additionally, we outline future experiments such as clicking the CPP to other biomolecules, labelling the cell surface of a cell through a metabolic labelling pathway (utilizing cell digestion to install the means of ligation), and investigating different sizes of CPPs for ligation purposes.

Acknowledgements

I would like to thank Dr. Ramesh Jasti for allowing me to accomplish the research discussed in this paper. Being a part of the lab has been a highlight of my undergraduate career and has taught me so much about chemistry, being a part of a team, collaborative work, and critical thinking. I also would like to thank Julia Fehr for being an incredible mentor during my undergraduate career. From teaching me every possible technique in lab, to helping me understand each chemical reaction, you have not only taught me about chemistry but how to be a hardworking, confident woman in science. I would like to thank Dr. Barbara Mossberg for your support in my honors college career. Your enthusiasm for learning has encouraged me in my journey as an undergraduate. I'd also like to acknowledge the Robert. D. Clark Honors College for expanding my knowledge outside of my field and providing me with a well-rounded education. Lastly, I'd like to thank my mom, Vivien, dad, Tom, and brother, Zach for motivating me, supporting me, and providing the best support system as I navigated college and the challenges I faced. I could not have accomplished the courses/grades/achievements I did without all of these important people in my life and I am sincerely grateful for everyone I have met in my undergraduate career.

Table of Contents

An Abstract of the Thesis of.....	ii
Acknowledgements	iv
Table of Contents	v
List of Figures.....	vi
Chapter 1: Background.....	1
I.I Bioorthogonal Chemistry.....	1
I.II Fluorophores.....	5
I.III Cycloparaphenylenes as Novel Fluorophores.....	7
Chapter 2: [9+1]CPP as a Bioorthogonal Fluorophore	11
II.I [n+1]CPPs	11
II.II Alkyne CPPs as Novel Fluorophore Scaffold.....	13
II.III Stability of [9+1]CPP.....	15
II.IV Clicking the [9+1]CPP to a Biomolecule	18
II.V Future Directions.....	20
Chapter 3: Materials and Methods	22
III.I Overview	22
III.II Reaction Procedures.....	22
III.III Purification.....	27
III.IV Characterization.....	28
III.V Materials	28
III.VI Experimental Results	29
Bibliography	37

List of Figures

Figure 1. Complexity of navigating a chemical reaction in a living cell	2
Figure 2. Strain-Promoted Alkyne-Azide Cycloaddition (SPAAC)	3
Figure 3. StrainViz calculations show increased local strain at the alkyne.....	4
Figure 4. Mechanism of SPAAC reaction.....	5
Figure 5. Fundamentals of Fluorescence ⁵	6
Figure 6. HOMO-LUMO Interactions with Corresponding Emission.....	7
Figure 7. [8]CPP	8
Figure 8. HOMO-LUMO Gap of Cyclic vs. Linear Paraphenylene ¹⁰	9
Figure 9. Size Dependent-Fluorescence of [n]CPPs ¹⁰	9
Figure 10. First Water-Soluble CPP ¹²	10
Figure 11. Alkyne-Containing CPPs	11
Figure 12. Modifications to [n+1]CPP	12
Figure 13. Synthetic Scheme of [9+1]CPP.....	14
Figure 14. Stability experiment with L-Glutathione	16
Figure 15. Stability Experiment at Physiological Temperature	17
Figure 16. (a) Scheme of [9+1]CPP clicked to azido sugar (b) Mass spectroscopy data confirming the conjugated [9+1]CPP with the azido sugar. (c) ¹ H NMR confirming conjugated [9+1]CPP with the azido sugar.	20
Figure 17. Metabolic labelling schema	21
Figure 18. Lithiation Addition.....	23
Figure 19. TES protection	24
Figure 20. Lithiation Borylation.....	24
Figure 21. Sonogashira Reaction.....	25
Figure 22. Macrocyclization.....	26
Figure 23. Deprotection and Aromatization.....	27

Chapter 1: Background

I.I Bioorthogonal Chemistry

The ability to study biomolecules in their native settings is an important step in learning about how biological systems function. There are pre-existing methods that allow us to look into biological systems such as genetically encoded fluorescent proteins (ex. GFP or “green fluorescent protein”) whose ubiquitous use was recognized with the 2008 Nobel Prize in Chemistry.¹ The limitations with the use of GFP and similar fluorescent proteins lie within the biomolecules that can be fluoresced (i.e. GFP cannot fluoresce post-transcriptionally modified molecules such as lipids, nucleic acids, and glycans). Bioorthogonal chemistry is an innovative combination of chemistry in biological settings that holds the potential to fluoresce these restricted biomolecules. It refers to a chemical reaction that can selectively occur inside a biological system without disrupting native processes.²

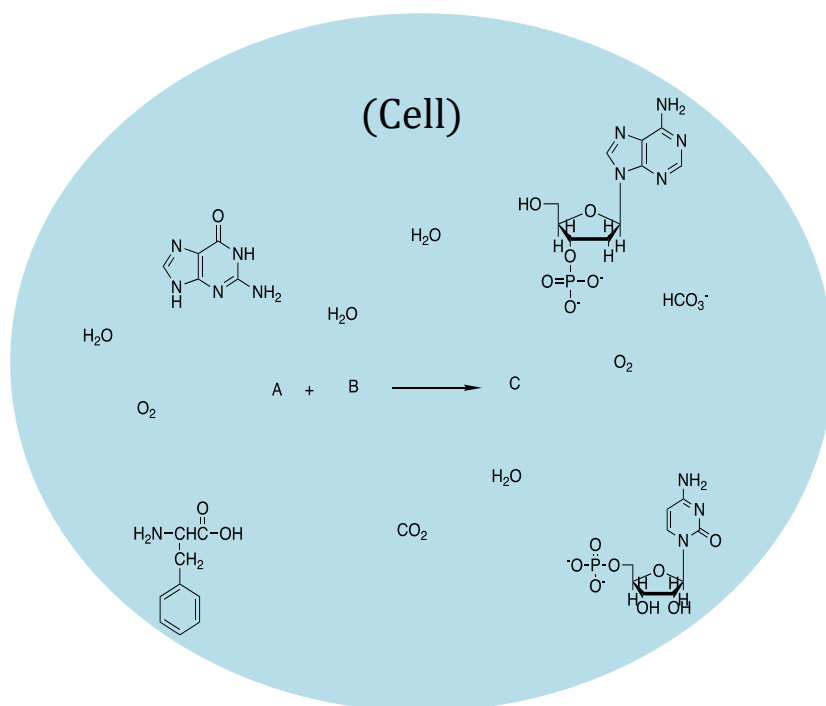


Figure 1. Complexity of navigating a chemical reaction in a living cell

When considering a bioorthogonal reaction, there are many requirements to fulfill. The first being that the reaction of interest must be selective. This means the components of the reaction will specifically react together without interfering with native biological molecules and processes. Figure 1 depicts the complexity of structures native to living systems and the chemical functional groups that must remain untouched. The second requirement is that the reaction must be kinetically favorable. This means the reaction must occur before any type of digestion/metabolization of the molecules of interest. Third is the reaction must have biological inertness; this means the two reactants and resulting product will not disrupt any biological processes. Lastly, the reaction must be biocompatible. This means the reaction must be non-toxic and

must function in biological conditions such as pH, aqueous environments, temperature, etc.

A common bioorthogonal ligation reaction is a reaction between an azide (N_3) and an alkyne (a carbon-carbon triple bond) through a [3+2] cycloaddition to form a triazole as depicted in Figure 2.

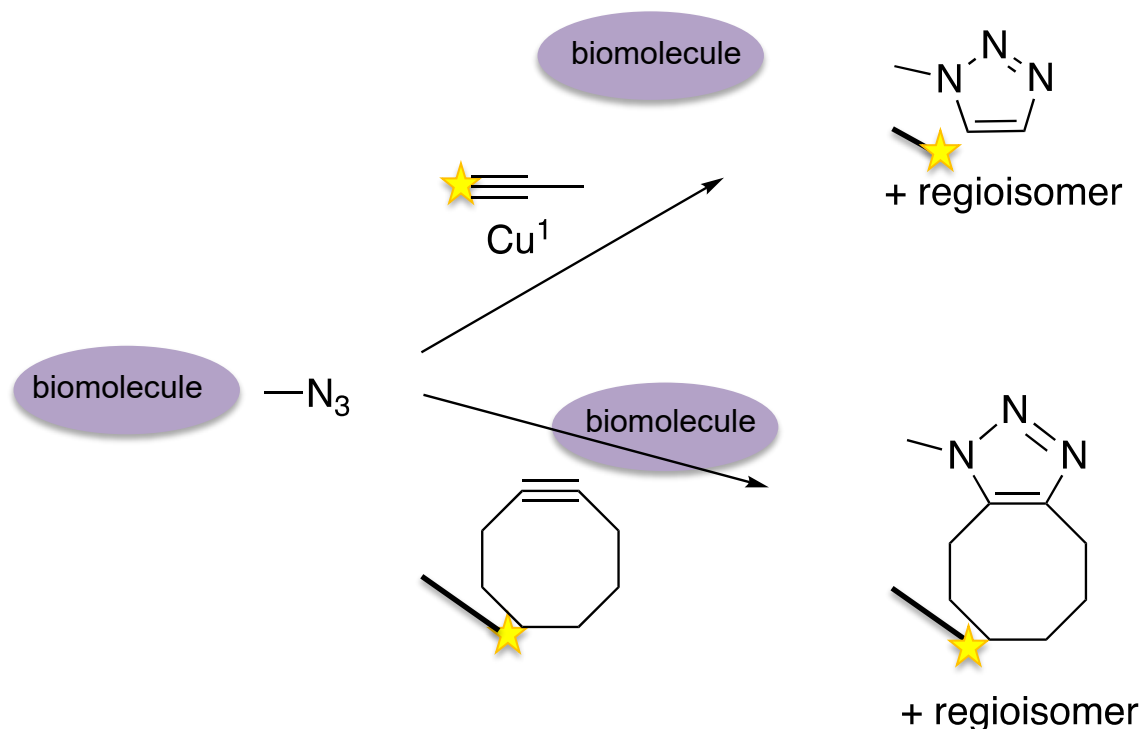


Figure 2. Strain-Promoted Alkyne-Azide Cycloaddition (SPAAC)

Generally, this ligation reaction occurs via a copper-catalyzed azide-alkyne cycloaddition reaction (CuAAC) *in vitro* (a reaction performed outside of a living system i.e. a test tube).³ However, when considering a bioorthogonal reaction, copper is extremely toxic to living systems. The Bertozzi group developed a copper-free click reaction to overcome the cytotoxicity of the copper². Instead of using $Cu(I)$ to activate the alkyne, the alkyne is instead introduced in a strained cyclooctyne where the ring strain destabilizes the alkyne. Not only does a cyclooctyne poses enough strain to drive

the reactivity, but so do other strained, cyclic alkyne molecules. The localized ring strain in an alkyne-containing CPP, discussed in more detail below, is depicted in Figure 3. This destabilization increases the reaction driving force, and likelihood of the strained alkyne to react and therefore relieve its ring strain.

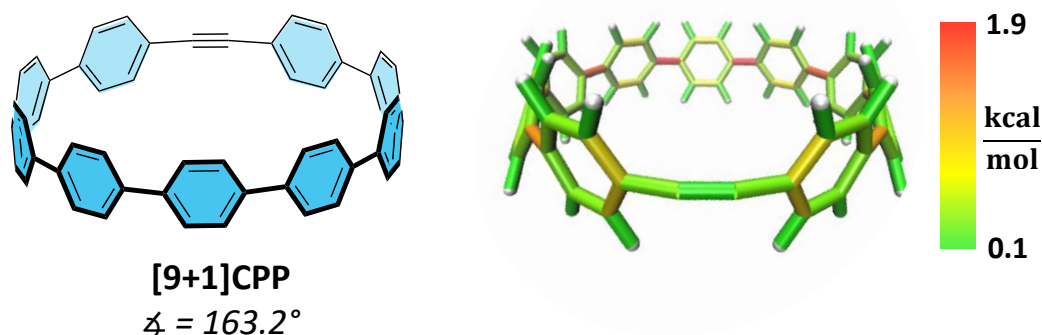


Figure 3. StrainViz calculations show increased local strain at the alkyne

The breakthrough discovery of the SPAAC reaction opens the doors for its use in bioorthogonal click reactions in living systems. The two components of this SPAAC reaction are the azide and the strained alkyne. The azide group is well suited for bioorthogonal reactions because it is extremely small and can easily permeate the cell membrane. It is metabolically stable and is not native to the cell which suggests that it would not interfere in any other reactions occurring in the cellular environment. In addition, the azide functional group has a unique resonance structure, as shown in the Figure 4, that provides a dipole moment. This distribution of electron density allows the nucleophilic alkyne to attack the non-charged nitrogen forming a more stable ringed structure.

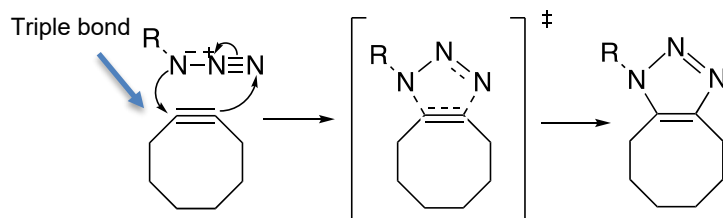


Figure 4. Mechanism of SPAAC reaction

The cyclooctyne is the other important counterpart of this reaction; the strain inherent to this molecule plays a unique role in facilitating the reaction. As shown in Figure 4, the cyclooctyne is a ring with a carbon-carbon triple bond embedded into its structure causing a great deal of ring strain (about 18 kcal/mol).⁴ An attractive aspect of the strained alkyne scaffold is that its structure can be manipulated to enhance reactivity, or even increase brightness and wavelength of the fluorescence.

I.II Fluorophores

Fluorophores, also called fluorescent molecules are critical for biological research. Their use allows researchers to detect the location and activation of proteins, visualize dynamic movement and changes in structures, detect environmental contaminants, and monitor biological systems. Fluorophores come in three different categories: proteins (i.e. GFP), synthetic polymers, or small organic molecules. As shown in Figure 5, fluorophores function by being “activated” when a photon of a very specific wavelength “excites” an electron in its ground state. The electron is then raised to an excited state where a portion of energy is dissipated to various sources until the

remaining energy emits in the form of a photon (i.e. fluorescent light), and the electron is returned to its ground state.

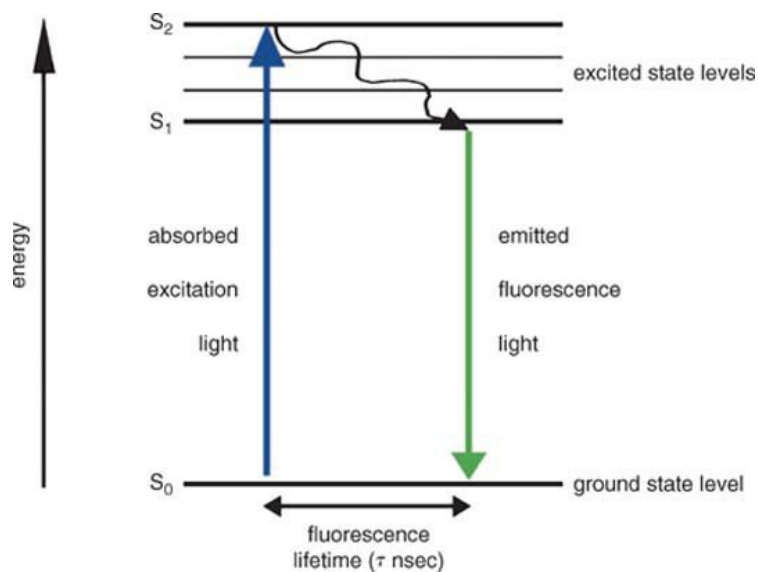


Figure 5. Fundamentals of Fluorescence⁵

There are two quantitative values that characterize the brightness of a fluorophore: the quantum yield and extinction coefficient. The quantum yield is the ratio of photons absorbed relative to the photons emitted through fluorescence. In other words, it characterizes the probability that the excited state electron will emit light when relaxing to the ground state level (as opposed to releasing the energy through a non-radiative mechanism). The extinction coefficient represents how well a molecule absorbs light at a certain wavelength. Combined, the two values represent how well a molecule absorbs and then re-emits light.

The emission color of the fluorophore relies on a molecular orbital interaction between the **Highest Occupied Molecular Orbital (HOMO)** and the **Lowest Unoccupied Molecular Orbital (LUMO)**. Orbitals systematically hold the electrons of a molecule and vary in energy level. The difference in energy between the HOMO and the LUMO,

also called the HOMO-LUMO gap, determines the color (or wavelength) of photon the fluorophore emits as shown in the figure below.

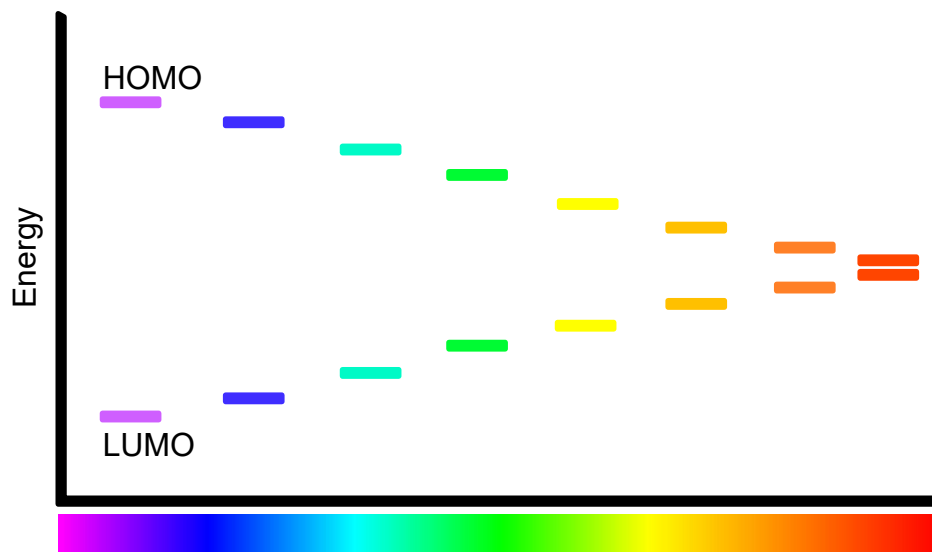


Figure 6. HOMO-LUMO Interactions with Corresponding Emission

Commonly used soluble organic dye fluorophores like photostable Fluorescein, Rhodamine, and Cyanine absorb from wavelengths ranging from 494 nm to 633 nm. The development of fluorophores is of great importance, as these small fluorescent molecules allow researchers to perform a myriad of biological analyses. Synthesizing new fluorophores with varying sizes and colors will help advance the biomedical field and our ability to learn and visualize living biosystems.

I.III Cycloparaphenylenes as Novel Fluorophores

Cycloparaphenylenes, also referred to as CPPs, are an appealing macromolecule for developing a new fluorophore. CPPs are a cyclic molecule made of varying numbers of benzene rings strung together in the *para*-position as seen in Figure 7.

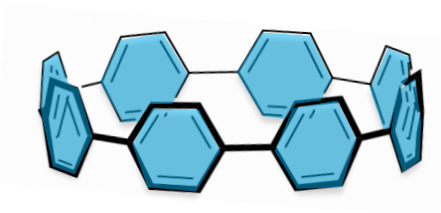


Figure 7. [8]CPP

Cycloparaphenylenes are controllably synthesized *via* stepwise organic synthesis. Their tunable syntheses allow for modifications to be made to the basic scaffold to enhance functionality. Current CPP research has been focused on modifying the basic structure of the ring to design synthetic polymers, rotaxanes, biological probes, and others.⁶⁻⁹

A very attractive feature of the CPP is its electronic and photophysical properties. Because of their tunable synthesis, CPPs can be synthesized with varying amounts (n) of phenyl groups ($[n]$ CPP). $[n]$ CPPs have a narrowing HOMO-LUMO gap as the number of phenyl groups decreases. This is a peculiar characteristic because non-cyclic (linear) paraphenylenes demonstrate the exact opposite trend, with an increasing HOMO-LUMO gap as the number of phenyl groups decreases (Figure 8).¹⁰

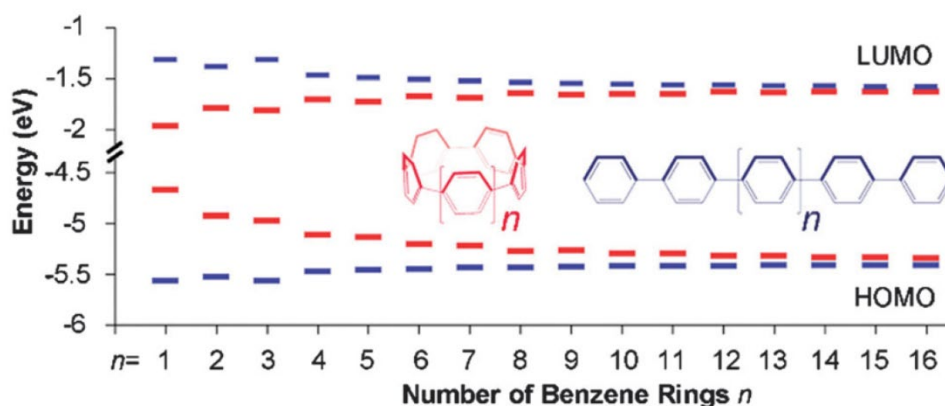


Figure 8. HOMO-LUMO Gap of Cyclic vs. Linear Paraphenylene¹⁰

Interestingly, CPPs share a common absorbance maximum while the emission is red shifted as the size of the hoop decreases (Figure 9).¹¹ Not only can their color be tunable, but their extinction coefficients and quantum yields are generally high, making several of them extremely bright. The optical properties of $[n]$ CPPs are an attractive feature, suggesting their potential to function as bioorthogonal fluorophores.

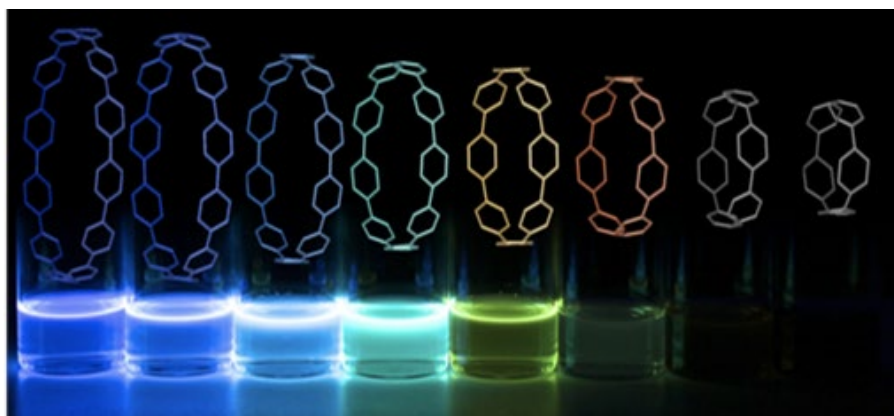


Figure 9. Size Dependent-Fluorescence of $[n]$ CPPs¹⁰

An essential requirement of a fluorophore is its compatibility with biological environments. As touched on before, the synthetic control of CPPs allows for modification to accommodate cellular environments. Figure 10 shows the first

established water-soluble CPP. It was proven to maintain the desirable optical properties of CPPs in aqueous buffer along with being non-toxic to living cells.¹² While it has been determined that the sulfonated [8]CPP has promising bioimaging capabilities, it did not actually link a CPP to a biomolecule. Further research is necessary to explore ways CPPs can selectively attach to biomolecules once inside a cell.

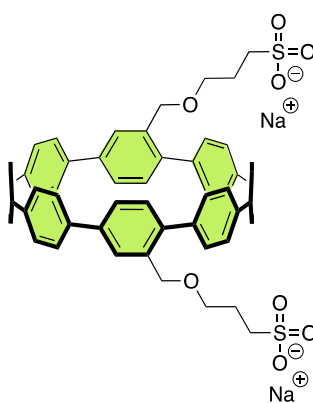


Figure 10. First Water-Soluble CPP¹²

These developments have uncovered a new subfield of research, focused on modifying the CPP scaffold and explore new ways it can be used as a biological tool. The next steps are investigating ways in which CPPs can be clicked to biomolecules and used in biological environments utilizing bioorthogonal chemistry such as the SPAAC reaction.

Chapter 2: [9+1]CPP as a Bioorthogonal Fluorophore

II.1 [n+1]CPPs

A new class of CPPs, also referred to as alkyne containing CPPs or [n+1]CPPs (*n* referring to the number of phenylenes in the molecule, '+1' referring to the addition of one alkyne unit) are extremely reactive due to their strained alkyne. Currently, [7+1]CPP, [9+1]CPP and [11+1]CPP have been synthesized and reported as seen in Figure 11.¹³

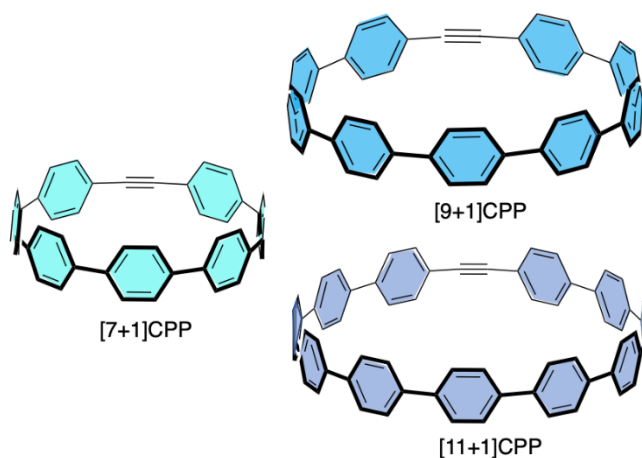


Figure 11. Alkyne-Containing CPPs

The benefit of incorporating the alkyne into the molecule is its high degree of reactivity. Alkynes have two pi bonds between two carbon atoms making them reasonably reactive in comparison to a completely saturated, non-pi bond-containing alkane. To add to the reactivity, incorporating the alkyne into a cyclic molecule like a cycloparaphenylene adds a great deal of ring strain to the alkyne. The “uncomfortable” geometry of the triple bond embedded into the ring drives the reactivity of the molecule so it can relieve its ring strain upon reacting with the azide.

$n+1$]CPPs can be synthesized with different modifications to further increase reactivity. A common means of modification is varying the size of the CPP. Figure 11 shows three different sizes of CPPs that have been synthesized. The smaller the CPP, (the fewer number of benzene rings incorporated) the more strained, and therefore reactive the molecule. In fact, the [7+1]CPP is so reactive that it is unstable at room temperature making it an undesirable option when considering its use as a fluorophore. A few other modifications of strained alkyne-containing CPPs are shown in Figure 12.

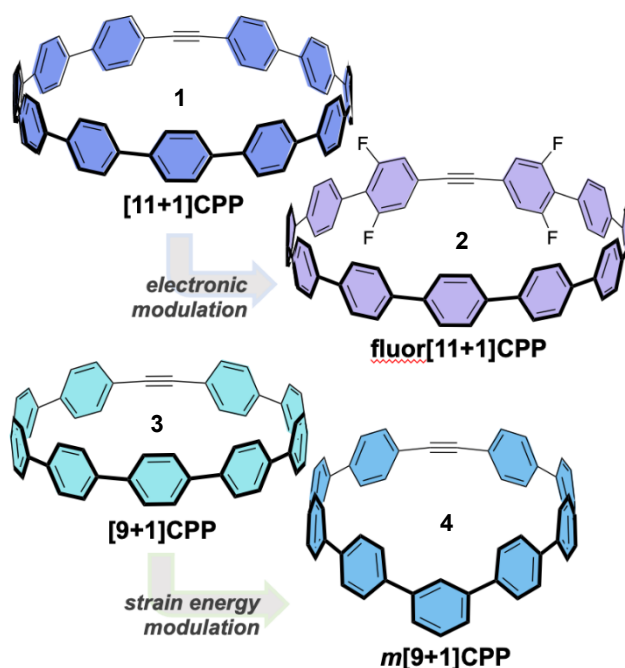


Figure 12. Modifications to [n+1]CPP

[11+1]CPP (**1**) is on the larger side of the group making the reactivity lower than that of a smaller size, such as the [9+1]CPP (**3**). However, this decrease in reactivity also comes with a significant improvement to its stability. Appending fluorine atoms *meta* to the alkyne (**2**) increases the reactivity of the molecule, without decreasing the size. The [9+1]CPP is a good middle ground in terms of size/reactivity and therefore stability.

Another interesting modification is introducing a different position of connectivity between benzene rings, such as the *meta* linkage, $m[9+1]$ CPP (**4**). This introduces a great deal of localized strain on the alkyne, resulting in an increase in reactivity.

II.II Alkyne CPPs as Novel Fluorophore Scaffold

What can these reactive alkyne CPPs be used for? As mentioned before, the strain-promoted azide-alkyne cycloaddition, also referred to as the SPAAC reaction, is a common means of chemical ligation (bringing together two molecules). A promising application of CPPs is their use in the SPAAC reaction as a substitute for the “strained cyclooctyne” reagent. This would involve conjoining a fluorescent molecule such as the $[n+1]$ CPP to a biomolecule (protein, sugar, DNA, etc.) that contains an azide. In theory, the azide and alkyne will react resulting in a linkage between the two, and therefore fluorescently tagging the biomolecule of interest.

The $[9+1]$ CPP is a promising candidate of the strained-alkyne CPP family for initial exploration as a bioorthogonal fluorophore. It fosters a good balance between reactivity and stability at room temperature. The synthesis of $[9+1]$ CPP involves starting with some commercially available materials and performing various reactions to build up to the macrocyclic molecule. The synthesis is shown in Figure 13.

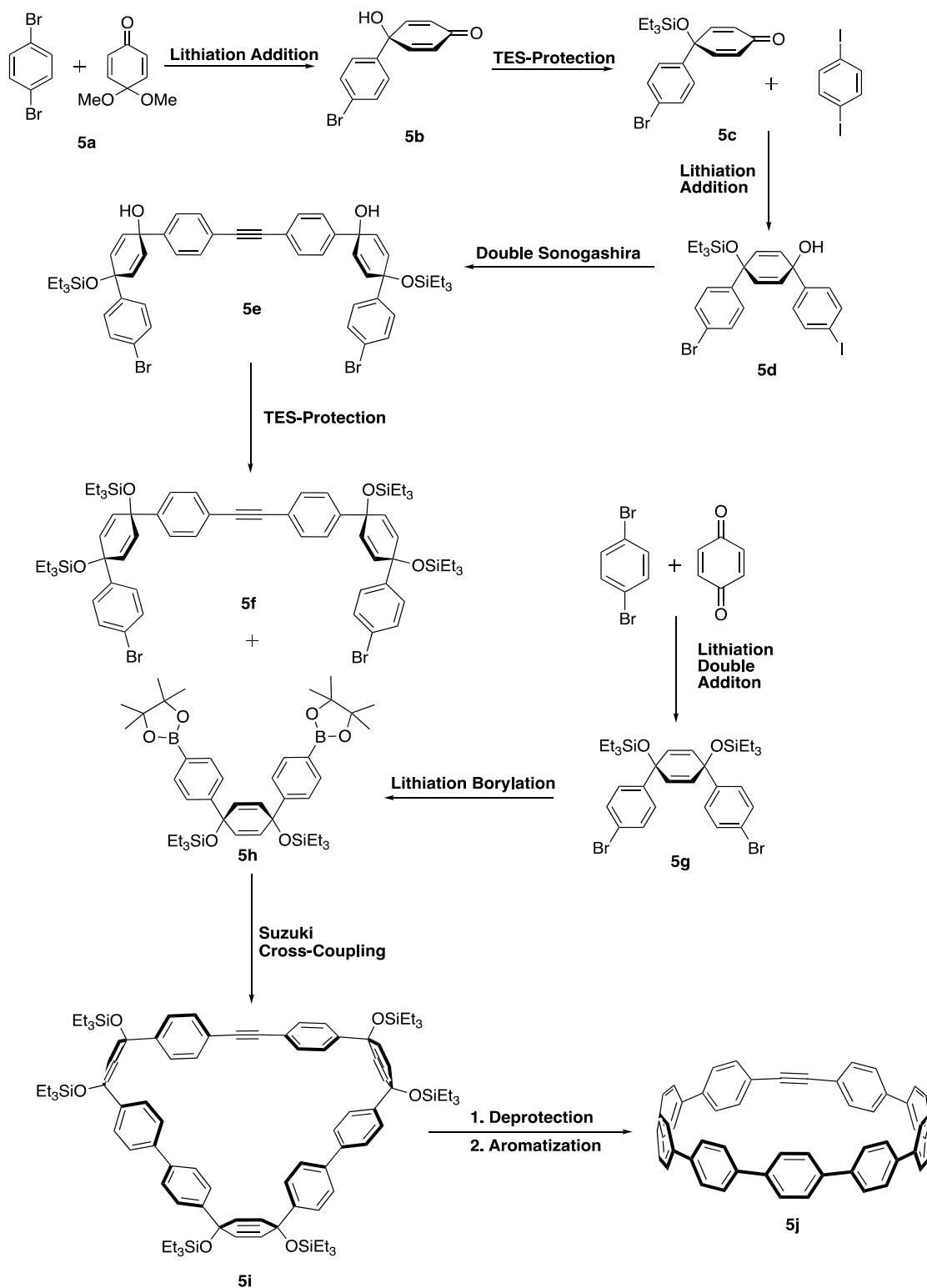


Figure 13. Synthetic Scheme of [9+1]CPP

The first step utilizes lithium-halogen exchange followed by nucleophilic addition to a ketone (see methods section) to create a carbon-carbon bond between the two starting materials (**5a-5b**). The TES-protection reaction adds large bulky protecting groups (triethylsilyl groups) to facilitate the *cis*-addition (**5c-5d**) and protect the alcohol (also called hydroxyl) group from any side reactions. The double Sonogashira reaction reacts two equivalents of **5d** with calcium carbide and various catalysts in a palladium- and copper-mediated cycle to install a carbon-carbon triple bond within the product (**5e**). Finally, an additional TES-protection is required to protect the hydroxyl groups and yield the first coupling partner of the [9+1]CPP, **5f**. The second coupling partner is synthesized in a similar matter, again utilizing lithium-halogen exchange with two equivalents of dibromobenzene and nucleophilic addition into a diketone (a so-called double addition) to afford **5g**. A lithium-halogen exchange followed by treatment with an electrophilic source of boronic ester replaces the bromine groups with boron-containing “Bpin” groups (**5f**); this is essential for the final cross-coupling reaction. Once both coupling partners are synthesized, a Suzuki cross-coupling reaction between organoboronic esters and halides creates the carbon-carbon bonds necessary to yield the macrocycle, **5i**. The final steps are to remove the TES groups (deprotect), remove the hydroxy groups, and install the missing double bonds to reform the benzene aromaticity (aromatize) and afford the finished [9+1]CPP.

II.III Stability of [9+1]CPP

With the [9+1]CPP synthesized, the first step in analyzing its potential as a bioorthogonal fluorophore is to explore the stability of the molecule. Because bioorthogonal reactions involve a reaction between two molecules in a living system,

the reaction must be extremely selective and stable in environments full of other biomolecules. To test the stability of the [9+1]CPP, we modelled our own experiment off of research done by the Prescher lab in 2018.¹⁴ The experiment was designed to model a biological environment *in vitro* by using a biological nucleophile, L-glutathione (GSH), and incubating it with [9+1]CPP. The reaction was monitored via ^1H NMR and the results are shown in Figure 14.

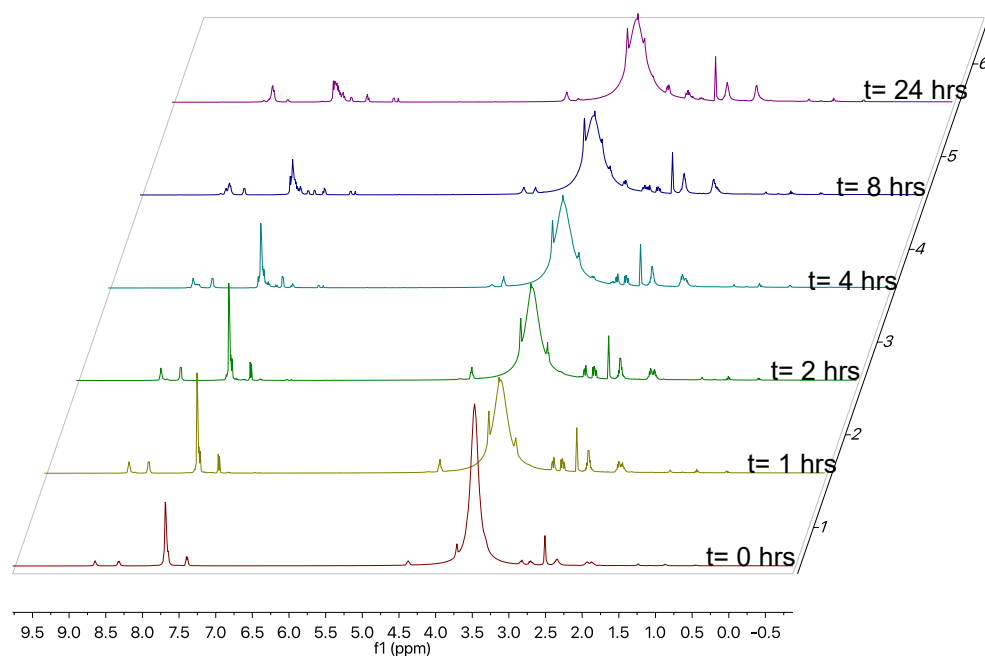


Figure 14. Stability experiment with L-Glutathione

The results show a series of ^1H nuclear magnetic resonance (NMR) scans at various time marks during incubation. Over the course of 24 hours, it appears that the [9+1]CPP reacted with a biological nucleophile present on GSH. After further investigation we found that [9+1]CPP reacted with a thiol group on GSH via a different click reaction. While these results show that—at higher concentrations—strained-alkyne CPPs could be susceptible to degradation by thiol-containing biological

nucleophiles, the minimal concentration of thiol groups in a standard cellular environment would likely not disrupt our bioorthogonal click reaction.

Our next stability experiment tested the stability of the [9+1]CPP at physiological temperature. This involved incubating the [9+1]CPP in dimethyl sulfoxide (DMSO) in a tube heated to physiological temperature (37 °C) over the course of 8 days and monitoring its degradation via ¹H NMR. The results are shown in Figure 15 below.

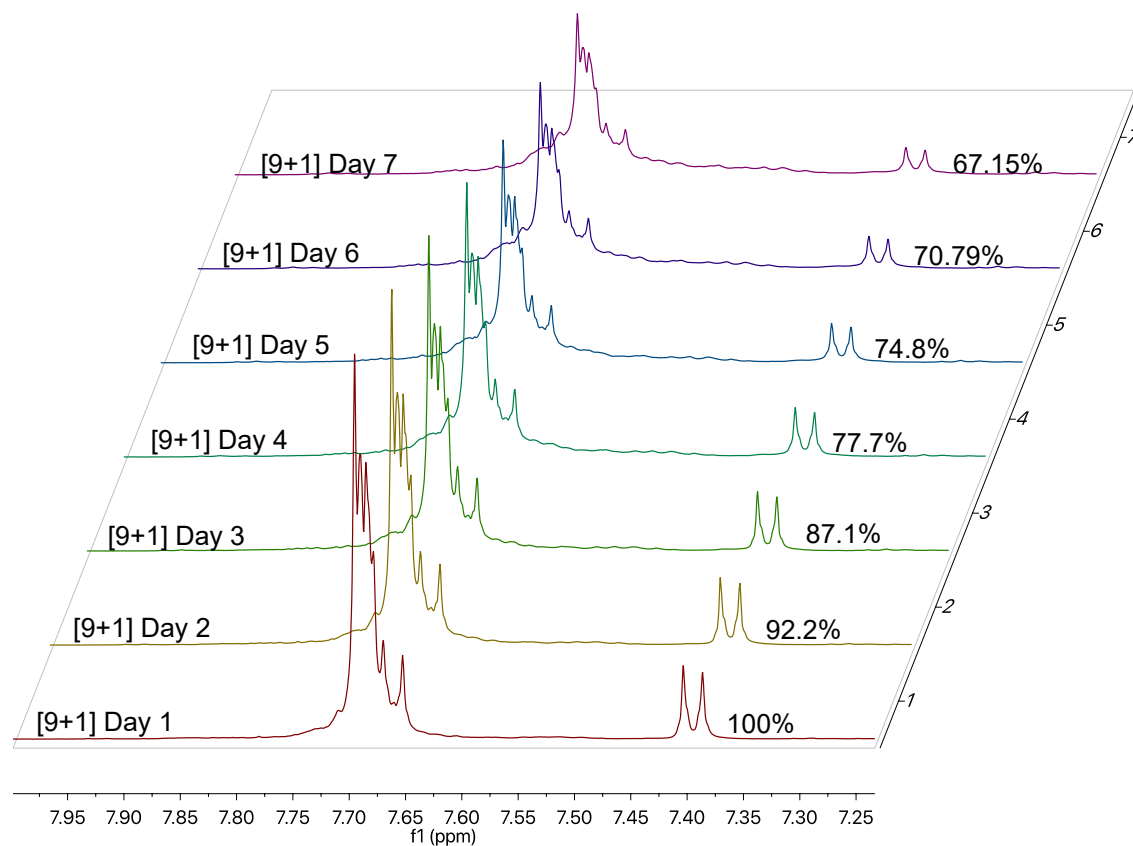


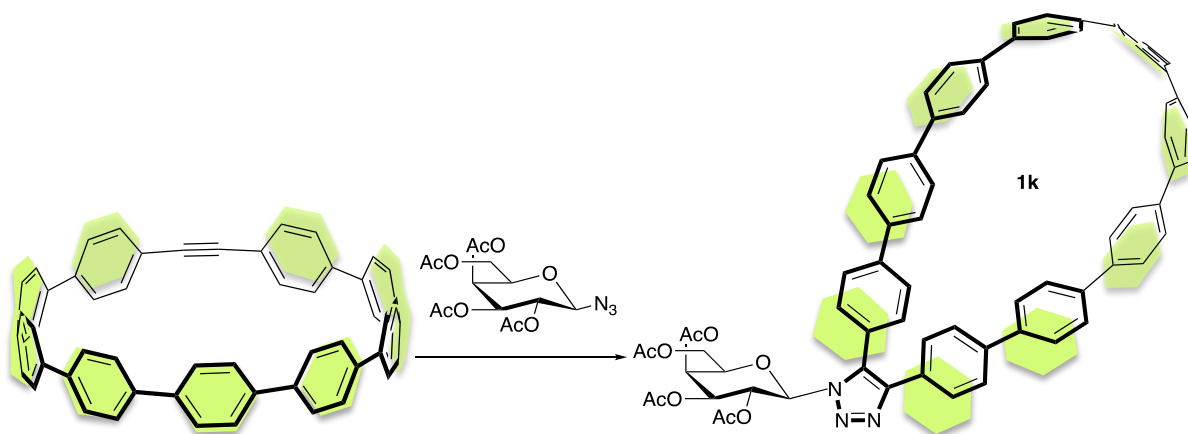
Figure 15. Stability Experiment at Physiological Temperature

The results of this experiment were promising. Minimal signs of degradation appeared after eight days of incubation at 37 °C which suggests medium-long term bench stability.

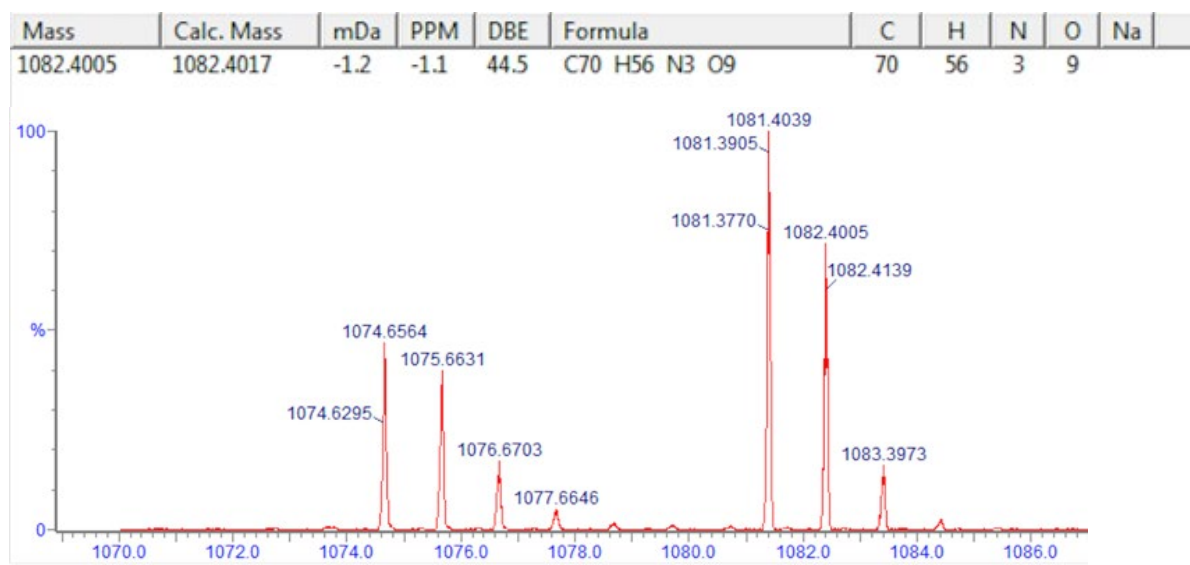
II.IV Clicking the [9+1]CPP to a Biomolecule

A long-term effort of cycloparaphenylene research has been to utilize their fluorescence in biological systems to tag and monitor biomolecules. The development of the family of strained-alkyne CPPs has led us to begin investigating its potential as a bioorthogonal fluorophore. The next step is testing to see if the [9+1]CPP is capable of clicking to a biomolecule through the SPAAC reaction. The biomolecule we chose was an azide-containing (azido) sugar called 1-Azido-1-deoxy- β -D-glucopyranoside tetraacetate. This sugar is equipped with acetyl groups which have proven to be cell permeable and digestible by cells along with an azide which is a key component in the SPAAC reaction. The [9+1]CPP was incubated in a flask with 1-Azido-1-deoxy- β -D-glucopyranoside tetraacetate for 48 hours at room temperature and the reaction was monitored via ^1H NMR. After 48 hours the reaction had run to completion and the product was analyzed. Both mass spectrometry (Figure 16b) and ^1H NMR (Figure 16c) confirmed the [9+1]CPP had clicked to the azido sugar (Figure 16a) and the product appeared pure as shown in Figure 16.

a



b



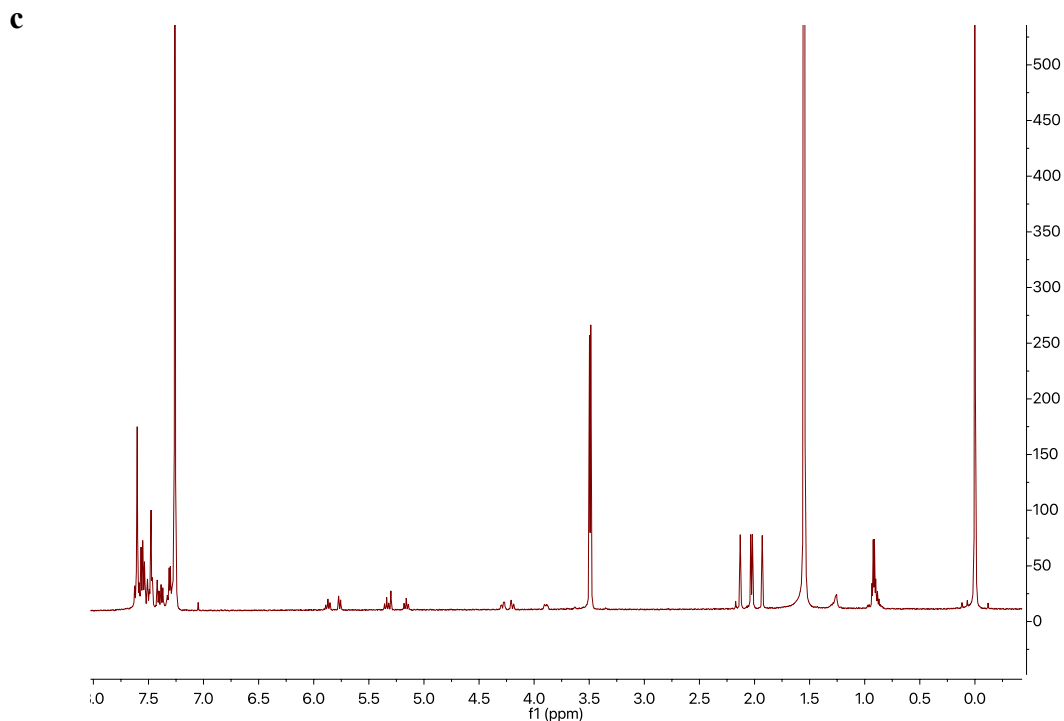


Figure 16. (a) Scheme of [9+1]CPP clicked to azido sugar (b) Mass spectroscopy data confirming the conjugated [9+1]CPP with the azido sugar. (c) ^1H NMR confirming conjugated [9+1]CPP with the azido sugar.

This is the first documented account of a strained-alkyne CPP-biomolecule conjugate as shown in Figure 16.

II.V Future Directions

With time as a limitation, not all projects could be finished for this report. With the successful demonstration of the [9+1]CPP as a stable fluorophore capable of clicking to a biomolecule *in vitro*, the next steps are to analyze its capability *in vivo* (i.e. in living cells). We plan to metabolically label glycoconjugates in living cells. This metabolic labelling procedure utilizes the cells biosynthetic machinery to digest azido sugars (specifically *N*-Azidoacetylmannosamine-tetraacylate) resulting in azides incorporated onto their cell surface. These exposed azides can serve as the means

of ligation with the [9+1]CPP to label the cell surface in living human cells. See Figure 17 for a scheme of the future metabolic labelling experiment.

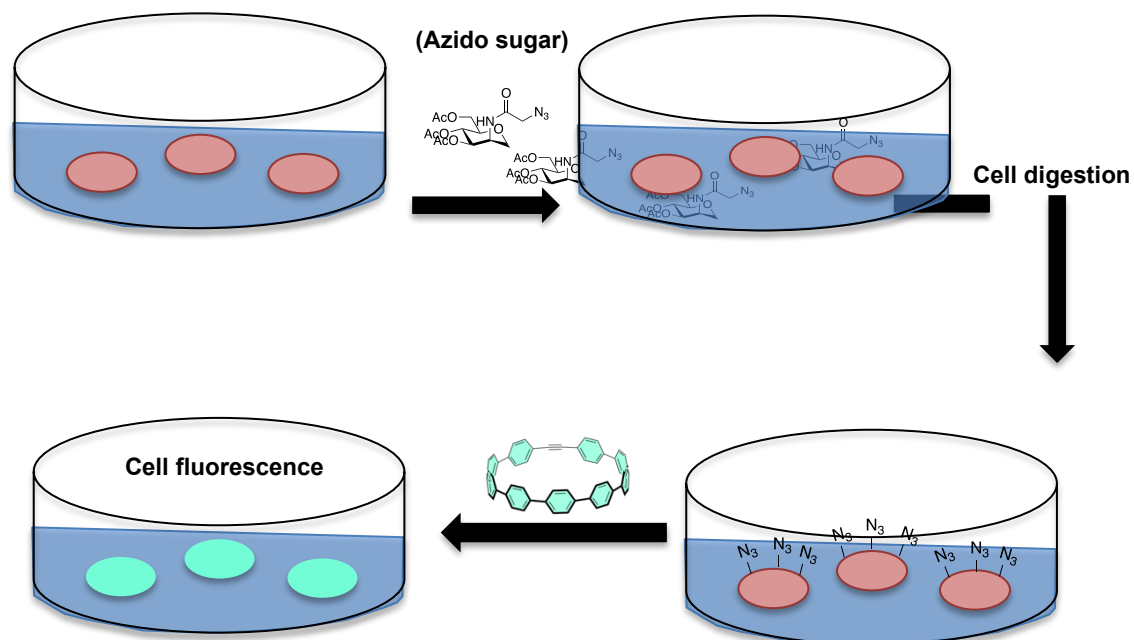


Figure 17. Metabolic labelling schema

The next phase we plan to do is to explore the reactivity and stability of the $m[9+1]$ CPP. Introducing more localized strain on the alkyne is sure to increase its reactivity but most likely will come with the burden of decreased stability. It will be interesting to see its comparison with the [9+1]CPP and whether one is a better candidate as a fluorophore. We also plan on exploring the ability of the [9+1]CPP to click to different biomolecules. Specifically, post-transcriptionally modified biomolecules that genetically encoded fluorophores are unable to fluoresce such as nucleic acids. Demonstrating the capability of strained alkyne-CPPs to click to a variety of biomolecules is crucial in establishing its ability to act as a widely applicable bioorthogonal fluorophore.

Chapter 3: Materials and Methods

III.I Overview

[9+1]CPP synthesis began with basic commercially-available materials. From these, various reactions were used to build upon their structure until they became large and functionalized. The large functionalized curved structures (coupling partners) were combined and coupled together to achieve a large cyclic structure (macrocycle). Two final reactions were performed to achieve the aromatic structure of the molecule. After synthesizing each molecule, a series of purification steps were executed which allowed the isolation of the product of interest from side products and starting material.

Purification techniques included extraction, filtration, thin layer chromatography, and column chromatography. After each building block was synthesized and purified, each molecule was characterized with ^1H NMR in order to confirm the reaction went to completion and the correct product was formed.

III.II Reaction Procedures

Unless otherwise stated, the following reactions were done in flame-dried (under vacuum) glassware and kept under an inert gas environment to avoid the accumulation of air or water that could contaminate the reaction. All solids were added to empty reaction flasks and placed under vacuum; the flask was then backfilled with an inert, unreactive gas (usually nitrogen gas). In addition, liquids were added to reaction flasks via a syringe and needle under inert atmosphere.

Lithiation-Addition

Lithiation-addition is a colloquial term for a reaction that involves two primary steps: a lithium/halogen exchange followed by nucleophilic addition into a ketone. The combination of these two steps is a foundational reaction in the synthesis of CPPs as it connects two rings together and forms a new carbon-carbon bond. The lithium/halogen exchange requires the reagent *n*-butyllithium to react with an aryl halide in a solution of tetrahydrofuran (THF) at $-78\text{ }^{\circ}\text{C}$. This is followed by the dropwise addition of a ketone substrate (such as the ketone shown in Figure 18) and stirring for 1 hour. The reaction is then quenched with deionized water and the product is purified.

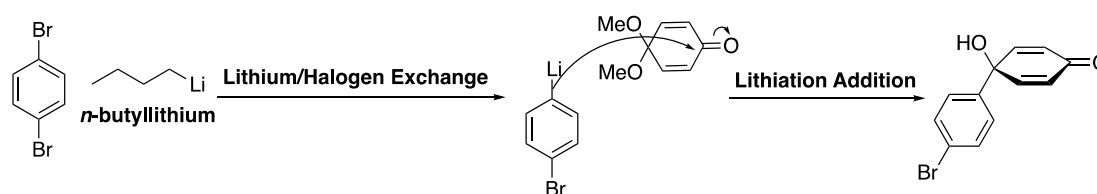


Figure 18. Lithiation Addition

TES Protection

Triethyl silyl (TES) protection reactions are a unique way to force a stereoselective addition to one face of the molecule (*cis*-addition). This ensures the molecule retains its curved nature which is needed for the cyclic CPP structure. The reaction involves installing TES groups onto structures containing hydroxy groups (OH groups). This is done by combining the hydroxy containing structure with imidazole in dimethylformamide. Chlorotriethylsilane is then added to the solution and allowed to stir at $40\text{ }^{\circ}\text{C}$ overnight. After the reaction has run to completion it is quenched with sodium bicarbonate.

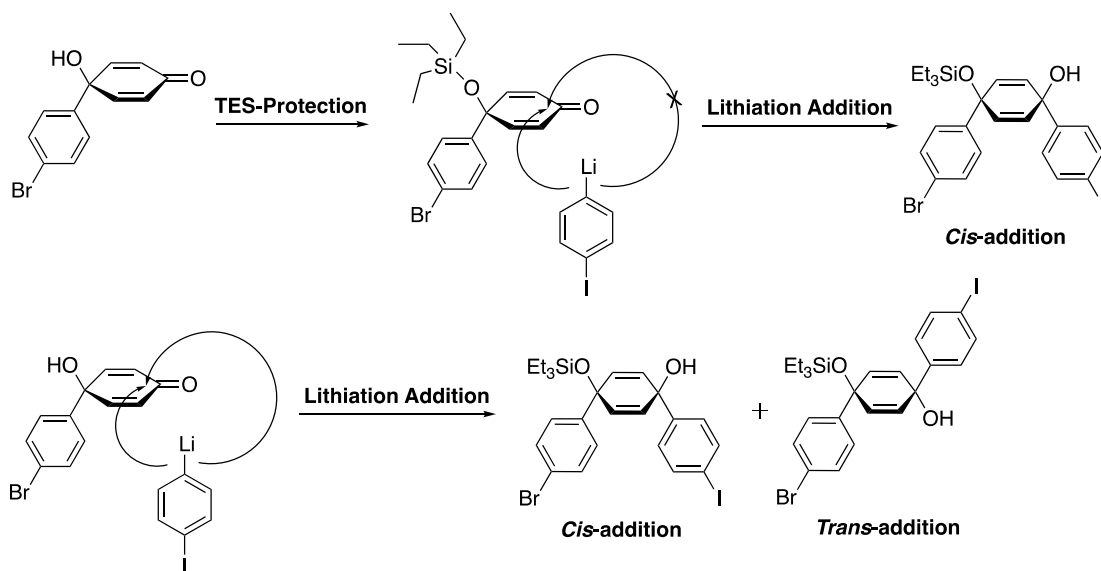


Figure 19. TES protection

Lithiation-Borylation

The Lithiation-Borylation follows a very similar mechanism as the lithiation-addition. The mechanism starts with a standard lithium/halogen exchange with *n*-butyllithium. The second step is adding into isopropoxy-Bpin, an electrophilic source of boronic ester (Bpin). Installing the Bpin groups is essential for the future Suzuki cross coupling reaction (shown in Figure 22).

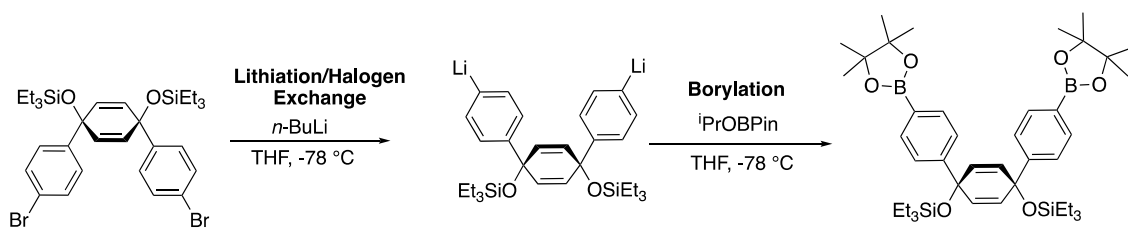


Figure 20. Lithiation Borylation

Sonogashira Reaction

The Sonogashira reaction is a palladium-catalyzed reaction that creates a carbon-carbon bond between two starting materials: a terminal alkyne and a halogen-containing molecule. The ‘double’ Sonogashira simply does this twice by adding functionality on both sides of the carbon-carbon triple bond as shown in Figure 20. The reaction utilizes calcium carbide which is activated by water to provide the carbon-carbon triple bond-containing acetylene molecule. The procedure involves adding water-containing (wet) acetonitrile, palladium acetate, triphenyl phosphine, copper iodide, and triethylamine to a flask, along with the coupling partners described above. This reaction is allowed to stir overnight at room temperature under inert atmosphere.

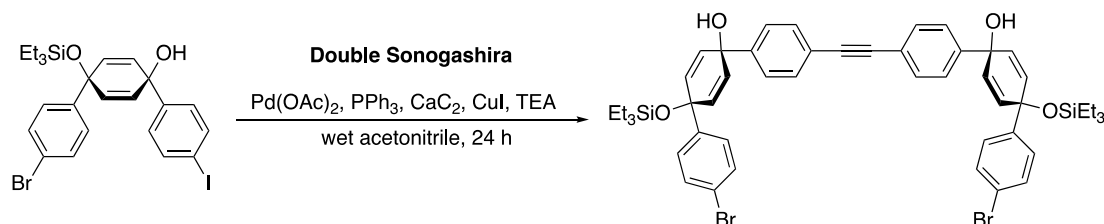


Figure 21. Sonogashira Reaction

Suzuki Macrocyclization

Suzuki macrocyclizations are another metal-catalyzed reaction that create carbon-carbon bonds between two molecules. Specifically for CPPs, they form what is called the “macrocycle” which is the protected and unaromatized version of the CPP. The reaction is designed to run in extremely dilute concentrations in order to force an intramolecular coupling (coupling within a single molecule) over the intermolecular coupling (coupling between two separate molecules) as shown in Figure 21.

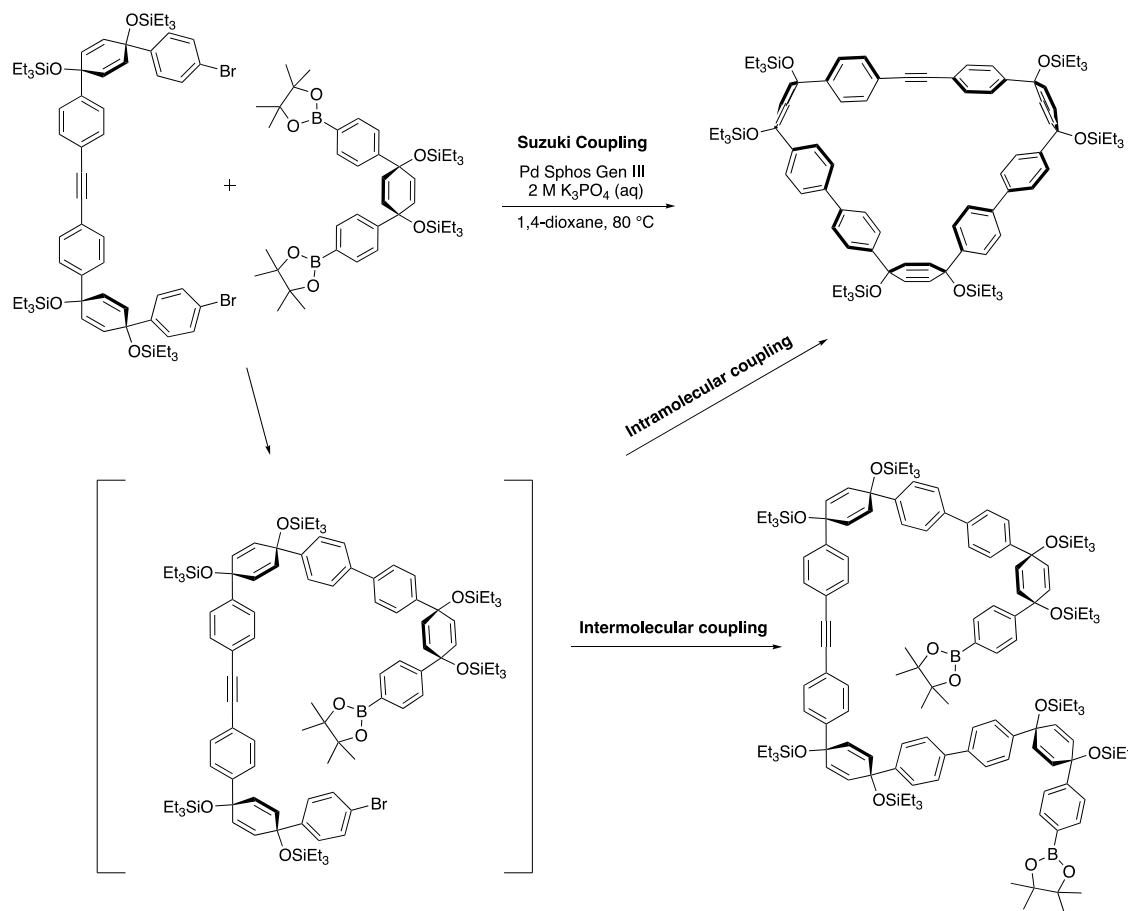


Figure 22. Macrocyclization

Deprotection and Aromatization

The last step before obtaining the CPP is to deprotect the macrocycle and aromatize the six-membered rings. Several TES protecting groups were used to force the curvature of the molecule; these are still present in the unaromatized macrocycle. The deprotection step uses tert-butyl ammonium fluoride to convert the TES groups into OH groups as shown in Figure 23. The final step then converts the cyclohexadienes into aromatic phenylenes *via* a tin-mediated reductive aromatization. The procedure involves combining the deprotected macrocycle with H_2SnCl_4 solution in THF at room temperature for one hour.

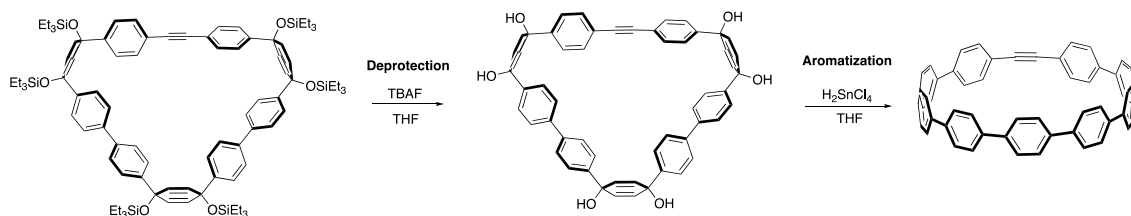


Figure 23. Deprotection and Aromatization

III.III Purification

Liquid Extraction

Extraction involves separating products and impurities based on solubility. It utilizes the different densities and immiscibility of select solvents to cleanly separate the different layers of solvent in a large funnel. The standard extraction protocol starts with dissolving the crude (unpurified) product in ethyl acetate (an organic solvent). Ideally the desired product would be soluble in the organic layer while the reaction byproducts will remain in the water layer (aqueous layer). Additional ethyl acetate is added to the aqueous layer, shaken, and the organic layer is combined with the previous organic fraction. This is repeated three times. The combined organic layers are then washed with brine three times to pull excess water out of the organic solvent; this aqueous layer is drained after each wash. Finally, sodium sulfate is added to the organic solution to remove any remaining water (usually referred to as ‘drying’ the solution) and the resulting solution is rotovapped (condensed) down to a more purified product.

Column Chromatography

Column chromatography, also known as flash chromatography, separates molecules based on polarity. It involves loading the crude (impure) product onto silica or alumina gel and washing down the column with solvents of varying polarity. The solvents that are used are picked carefully so they can strategically pull down the product from the column while keeping the impurities remaining in the gel. The resulting wash-through is then collected in small fractions and the product containing fractions are rotovapped (condensed) down.

Recrystallization

Recrystallization involves dissolving an impure product in a solvent it is minimally soluble in. Heat is commonly applied to increase solubility of the impure product in solution. The solution is then placed in the freezer which forces the pure product to crash out into a solid. The solid is then vacuum filtered and isolated.

III.IV Characterization

^1H (proton) NMRs were recorded at 500 MHz using Bruker Avance III 500 spectrometer. NMR samples were dissolved in CDCl_3 .

III.V Materials

Molecules were assembled using the commercially available starting materials as shown in Figure 23.

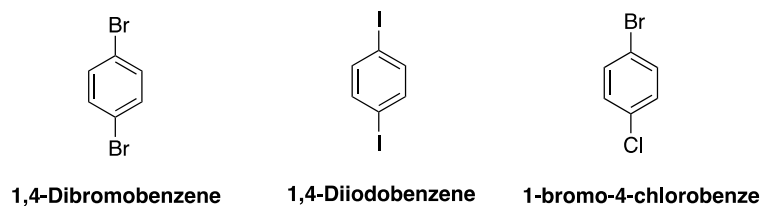
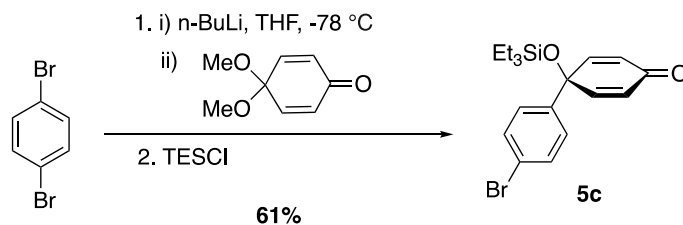


Figure 23. Substrate building blocks

Solvents

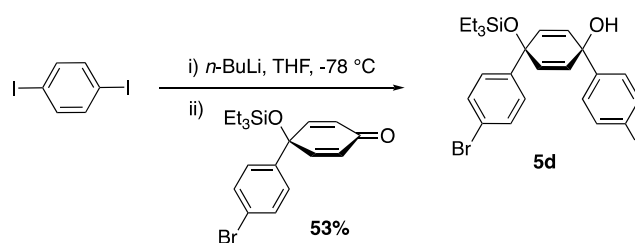
Each reaction was run in either tetrahydrofuran (THF), dimethylformamide (DMF), dichloromethane, 1,4-dioxane, or toluene. These solvents were stored in a PPT solvent purification system where they are run through a water extraction column and stored under argon gas to maintain purity and oxygen free. Additional solvents were used but stored under air.

III.VI Experimental Results



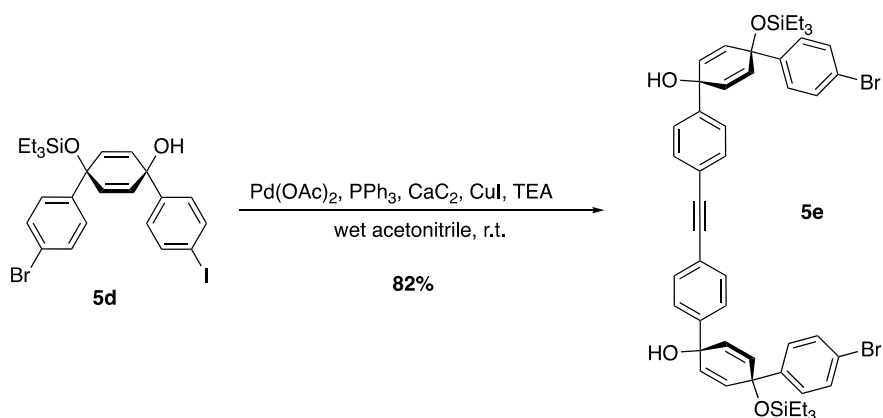
Synthesis of 5c. a 500 mL flame dried round bottom flask equipped with a stir bar was charged with 1,4-dibromobenzene (25.2 g, 0.107 mol, 1.1 eq). The reaction flask was capped with a septum and evacuated and backfilled with nitrogen gas. To this, THF (139 mL, 0.7 mol/L) was added via syringe and the reaction flask was lowered into a $-78\text{ }^\circ\text{C}$ dry ice/isopropyl alcohol (IPA) bath and allowed to stir for 50 minutes. *n*-butyllithium (40.9 mL, 2.5 mol/L) was added to the solution dropwise. This was followed by the dropwise addition of 4,4-dimethoxycyclohexadienone or ketal (13.6

mL, 1.1 g/mL). The solution was allowed to stir for one hour in the dry ice/IPA bath before TESC1 (19.59 mL, 0.898 g/mL) was added. The solution was allowed to stir overnight and come to room temperature over this time. The reaction was then quenched with water (150 mL) and sodium bicarbonate (120 mL), extracted with hexanes (3x100 mL), and washed with brine (3x100 mL). The product as then dried with sodium sulfate and concentrated down to yield an orange oil. The crude oil was purified via a silica column (30% dichloromethane/hexanes) to yield a lighter yellow oil (22.51 g, 61%). ¹H NMR (500 MHz, Chloroform-*d*) δ 7.57 – 7.42 (m, 1H), 7.37 – 7.28 (m, 1H), 6.83 – 6.73 (m, 1H), 6.27 – 6.18 (m, 1H), 0.97 (t, *J* = 7.9 Hz, 4H), 0.66 (q, *J* = 7.9 Hz, 3H).



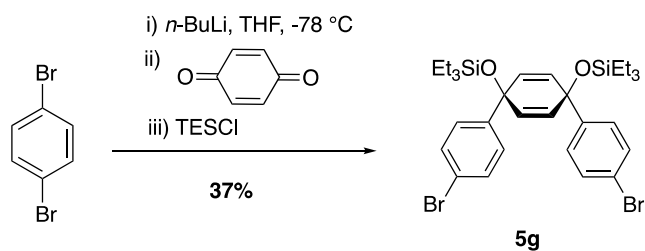
Synthesis of 5d. 1,4-diodobenzene (3.3g, 0.01 mol, 1.25 eq) was added to a 100 mL flame-dried round bottom flask equipped with a stir bar. To this, THF (26.6 mL, 0.3 mol/L) was added to the flask and the solution was placed in a dry ice/IPA bath at -78 °C and allowed to stir for 45 minutes. *n*-butyllithium (4 mL, 2.3 mol/L) was added dropwise to the flask and allowed to stir for 5 minutes. Bromoketone **5c** (2.75 mL 7.98 mmol, 1 eq) was added dropwise. The reaction was allowed to stir for one hour and then quenched with deionized water. The solution was then removed from the ice bath and allowed to warm to room temperature. It was then extracted with ethyl acetate (3x50

mL), washed with brine (3x40 mL), dried over sodium sulfate, and concentrated down. The resulting product was an orange viscous oil. The crude oil was purified by running through a silica column (10% ethyl acetate/hexanes) to yield a light orange oil (2.45 g, 53%). ¹H NMR (500 MHz, Chloroform-*d*) δ 7.72 – 7.65 (m, 1H), 7.44 – 7.38 (m, 1H), 7.24 – 7.19 (m, 1H), 7.19 – 7.14 (m, 1H), 2.02 (s, 1H), 0.99 (t, *J* = 7.9 Hz, 4H), 0.68 (q, *J* = 7.9 Hz, 3H).



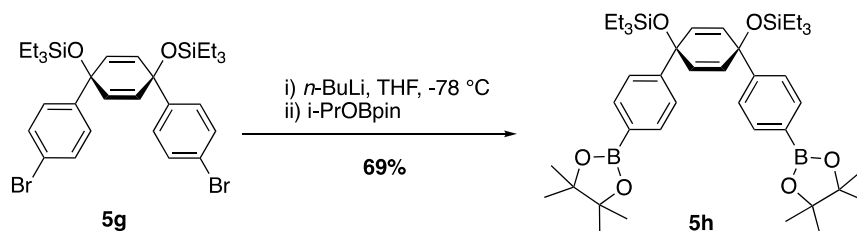
Synthesis of 5e. Wet acetonitrile (20.99 mL, 0.2 mol/L) was added to a 50 mL round bottom flask and allowed to sparge under nitrogen gas for 40 minutes. Triphenylphosphine (0.055 g, 0.21 mmol, 0.05 eq), copper iodide (0.04 g, 0.21 mmol, 0.05 eq) and palladium (II) acetate (0.019 g, 0.083 mmol, 0.02 eq) were combined in a different 100 mL round bottom flask. **5d** (2.45 g, 4.3 mmol, 1 eq) was added to an additional 10 mL round bottom flask. The acetonitrile was used to dissolve the solids in the catalyst flask (15 mL) and a small amount (5 mL) was used to dissolve **5d**. The solution containing **5d** was added to the catalyst-containing flask. Lastly, triethylamine (1.75 mL, 0.72 g/mL), calcium carbide (0.81 g, 0.01 mol, 3 eq), and DI water (3 mL) were added to the reaction flask and the flask was allowed to stir overnight under nitrogen atmosphere. Dichloromethane (15 mL) was added to the reaction flask and

sonicated briefly. The reaction flask was run through a celite plug (washed with 300 mL of dichloromethane) and dried over sodium sulfate. The solution was concentrated down to yield an orange oil (1.6 g, 81.5%) ^1H NMR (500 MHz, Chloroform-*d*) δ 7.52 (d, $J = 8.1$ Hz, 1H), 7.42 (dd, $J = 8.6, 3.0$ Hz, 1H), 7.26 (s, 3H), 6.11 – 5.95 (m, 2H), 1.48 (t, $J = 7.3$ Hz, 3H), 1.00 (t, $J = 7.9$ Hz, 3H), 0.69 (q, $J = 7.9$ Hz, 3H).



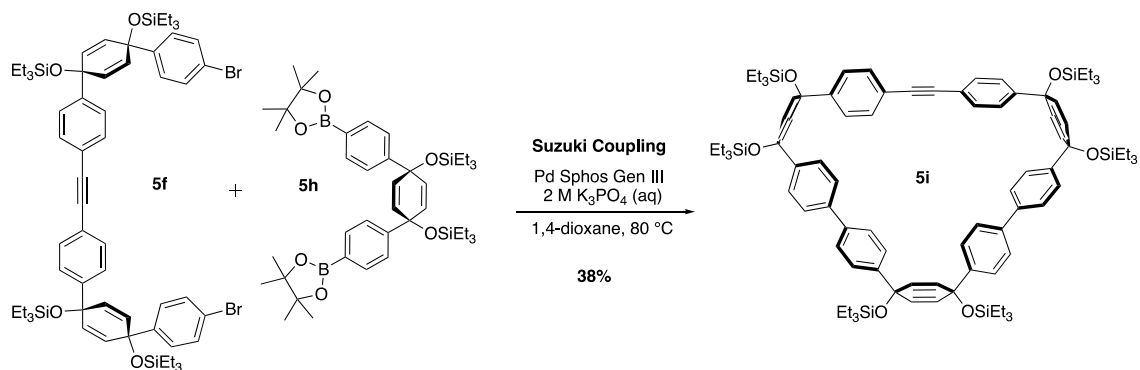
Synthesis of 5g. 1,4-dibromobenzene (6.35 g, 0.027 mol, 2.6 eq) was added to a 500 mL flame-dried three-neck round bottom flask equipped with a stir bar and a flame dried 125 mL addition column. THF (150 mL, 0.89 g/mL) was added via cannula and the reaction flask was allowed to stir in a -78 °C IPA/dry ice bath for one hour under nitrogen environment. *n*-butyllithium (10.77 mL, 2.28 mol/L, 2.3 eq) was added dropwise to the solution. *p*-benzoquinone (1.15 g, 0.011 mol, 1 eq) was dissolved in THF (21 mL, 0.89 g/mL) and added to the addition column. The addition column was opened to allow the dropwise addition of the solution into the reaction flask. The reaction was allowed to stir in the IPA/dry ice bath for 1 hour. TESCl (5.37 mL, 0.898 g/mL, 3 eq) was added to the reaction flask. It was then removed from the ice bath and allowed to warm to room temperature overnight. The reaction was then transferred into a 1 L RBF the next morning and DI water (100 mL) was added. The solution was then concentrated down, extracted with ethyl acetate (3x100 mL), washed with HCl (1x 40

mL, 2 mol/L), washed with brine (2 x 100 mL), and dried over sodium sulfate. The product was concentrated down to yield a dark brown oil. The crude product was further purified *via* silica column (3% ethyl acetate/hexanes) and concentrated down. The product was then sonicated in methanol (10 mL) which crashed out a white powder. The solid was collected via vacuum filtration (2.6 g, 37%). ¹H NMR (500 MHz, Chloroform-*d*) δ 7.41 – 7.36 (m, 1H), 7.20 – 7.13 (m, 1H), 0.92 (t, *J* = 7.9 Hz, 4H), 0.59 (q, *J* = 7.9 Hz, 3H).



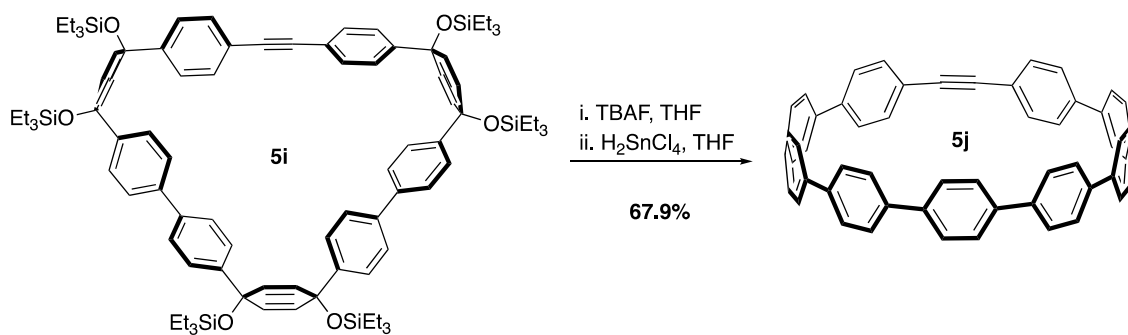
Synthesis of 5h. **1g** (1.3 g, 2 mmol, 1 eq) was added to a flame-dried 50 mL round bottom flask. THF (10.0 mL, 0.89 g/mL) was added to the flask and allowed to mix until the solid was dissolved. The solution was placed in a -78 °C IPA/dry ice bath and allowed to stir for 45 minutes. *n*-butyllithium (1.92 mL, 2.4 mol/L, 0.2 eq) was then added dropwise followed by the dropwise addition of ⁱPrOBpin (1.22 mL, 0.91 g/mL, 3 eq). The solution was then allowed to stir in the dry ice/IPA bath for 1 hour before it was quenched with DI water (20 mL) and allowed to warm to room temperature. The solution was extracted with dichloromethane (3x100 mL) and the organic layers were washed with water (2x75 mL) and brine (2x75 mL). The solution was then filtered and concentrated down to yield a clear oil. The oil was sonicated in methanol which afforded a white powder which was collected via vacuum filtration (1.03 g, 69%). ¹H

NMR (500 MHz, Chloroform-*d*) δ 7.75 – 7.64 (m, 1H), 7.39 – 7.28 (m, 1H), 0.92 (t, J = 7.9 Hz, 4H), 0.59 (q, J = 7.9 Hz, 3H).



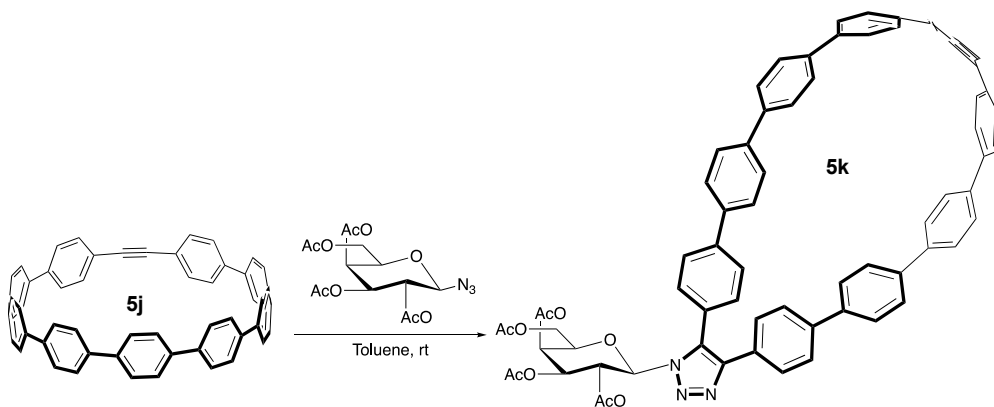
Synthesis of 5i. **5h** (0.28 g, 0.38 mmol, 1.1 eq), **1e** (0.4 g, 0.34 mmol, 1 eq) and Pd SPhos-Gen 3 (0.027 g, 0.034 mmol, 0.1 eq) were combined in a flame-dried 250 mL round bottom flask. The flask was evacuated and backfilled with nitrogen gas 5 times in order to ensure an air-free environment. 1,4-dioxane (168 mL) was added to a separate 250 mL flame dried flask and sparged with nitrogen for 60 minutes. The 1,4-dioxane was then added to the reaction flask and the flask was sparged with nitrogen for an additional 20 minutes. The reaction flask was then placed in an 80 °C oil bath and allowed to stir under nitrogen for 10 minutes. Aqueous K₃PO₄ (16.77 mL, 2 mol/L) was allowed to sparge for an hour, and then added to the reaction. The reaction was allowed to stir overnight in the 80 °C oil bath. The reaction was then removed from the oil bath and allowed to cool to room temperature. The solution was run through a celite plug (washed with 100% DCM, 300 mL). The resulting wash through was concentrated down and extracted with ethyl acetate (3x100 mL), washed with water (1x75 mL), and washed with brine (2x75 mL). The crude oil was then sonicated in acetone to yield a light-yellow solid and was collected via vacuum filtration (0.195 g, 38%). ¹H NMR

(500 MHz, Chloroform-*d*) δ 7.61 – 7.55 (m, 1H), 7.55 – 7.51 (m, 1H), 7.51 – 7.46 (m, 2H), 7.46 – 7.42 (m, 1H), 7.36 – 7.30 (m, 2H), 1.38 – 1.21 (m, 9H), 1.02 – 0.83 (m, 23H), 0.71 – 0.51 (m, 11H).



Synthesis of 5j. **5i** (0.165 g, 0.097 mmol, 1 eq) was added to a flame dried 50 mL round bottom flask. THF (12.09 mL, 0.948 g/mL) was added to the reaction flask to dissolve the solid. TBAF (0.639 mL, 1.0 mol/L) was then added dropwise to the solution and the solution was allowed to stir at room temperature for 1 hour under nitrogen environment. The solution was then concentrated down and sonicated in DI water (25 mL). The resulting solid was then collected via vacuum filtration and added to a flame-dried 50 mL flask. In a separate flame-dried 50 mL round bottom flask SnCl₂ (0.181 g, 0.8 mmol, 1 eq) was dissolved in THF (20 mL, 0.89 g/mL). HCl (0.13 mL, 12 mol/L) was added dropwise and the solution was allowed to stir at room temperature for 30 minutes. The resultant H₂SnCl₄ (4.29 mL, 0.04 mol/L) was then added to the flask containing the deprotected macrocycle. The reaction was allowed to stir at room temperature for 1 hour. The solution was then diluted with hexanes (40 mL) and run through an aluminum plug (50% DCM/Hexanes, 500 mL). The flow through was then concentrated down in a scint vial. The solid was sonicated in minimal ether and vacuum

filtrated. It was then dissolved in minimal DCM and sonicated down to yield a bright yellow powder (0.023 g, 67.9%) ^1H NMR (500 MHz, Chloroform-*d*) δ 7.59 (d, $J = 3.2$ Hz, 1H), 7.57 (d, $J = 3.4$ Hz, 1H), 7.55 (s, 1H), 7.53 (s, 1H), 7.52 (s, 1H), 7.37 (d, $J = 8.3$ Hz, 1H), 3.54 – 3.46 (m, 5H), 1.23 (td, $J = 7.0, 1.2$ Hz, 7H), 0.94 – 0.88 (m, 2H).



Synthesis of 5k. *5j* (0.0012 g, 1.69 μmol , 1 eq) was added to a 50 mL round bottom flask. Azido sugar (0.6 mg, 1.67 μmol , 1 eq) was added to the reaction flask. The flask was then evacuated and backfilled with nitrogen and toluene (1mL) was added to the flask. The flask was then lowered into a 40 $^{\circ}\text{C}$ oil bath and allowed to stir for 24 hours. The reaction was then concentrated down and sonicated in methanol to afford a bright yellow solid. ^1H NMR (500 MHz, Chloroform-*d*) δ 7.64 – 7.46 (m, 9H), 7.40 (dd, $J = 17.4, 8.1$ Hz, 2H), 7.31 (t, $J = 7.0$ Hz, 2H), 5.33 (dd, $J = 19.3, 9.8$ Hz, 2H), 3.49 (d, $J = 5.4$ Hz, 5H), 2.13 (s, 1H), 2.03 (d, $J = 7.5$ Hz, 2H), 1.93 (s, 1H), 1.26 (s, 1H), 0.95 – 0.84 (m, 4H).

Bibliography

1. The Nobel Prize – US http://nobelprize.org/nobel_prizes/chemistry/web. (Accessed Feb. 11, 2022)
2. Sletten, E. M.; Bertozzi, C. R. Angew. Bioorthogonal Chemistry: Fishing for Selectivity in a Sea of Functionality. *Chem. Int. Ed.* **2009**, *48*, 6974-6998. <https://doi.org/10.1002/anie.200900942>
3. Baskin, J. M.; Prescher, J. A.; Laughlin, S. T.; Agard, N. J.; Chang, P. V.; Miller, I. A.; Lo, A.; Codelli, J. A.; Bertozzi, C. R. Copper-free click chemistry for dynamic in vivo imaging. *Proceedings of the National Academy of Sciences.* **2007**, *104* (43), 16793-16797. doi:10.1073/pnas.0707090104
4. Huisgen, R. *Proc. Chem. Soc.* **1964**, 357-396.
5. Bach, R.; Ring Strain Energy in the Cyclooctyl System. The Effect of Strain Energy on [3+2] Cycloaddition Reactions with Azides. Journal of the American Chemical Society. *ACS Cent. Sci.* **2009**, *131*, 5223-5243. <https://doi.org/10.1021/ja8094137>
6. Lleres, D.; Swift, S.; Lamond, A.; Detecting Protein-Protein Interactions In Vivo with FRET using Multiphoton Fluorescence Lifetime Imaging Microscopy (FLIM) *Curr. Protocol. Cytom.* **2007**, 1934-9300. doi:10.1002/0471142956.cy1210s42
7. White, B. M.; Zhao, Y.; Kawashima, T. E.; Branchaud, B. P.; Pluth, M. D. Expanding the Chemical Space of Biocompatible Fluorophores: Nanohoops in Cells. *ACS Cent. Sci.* **2018**, *4*, 1173-1178. <https://doi.org/10.1021/acscentsci.8b00346>
8. Van Raden, J. M.; White, B. M.; Zakharov, L. N.; Jasti, R. Nanohoop Rotaxanes via Active Metal Template Syntheses and Their Potential in Sensing Applications. *Angew. Chem. Int. Ed.* **2019**, *58*, 7341-7345. <https://doi.org/10.1002/anie.201901984>
9. Leonhardt, E. J.; Jasti, R. Emerging Applications of Carbon Nanohoops. *Nat. Rev. Chem.* **2019**, *3*, 672-686. <https://doi.org/10.1002/anie.201901984>
10. Maust, R. L.; Li, P.; Shao, B.; Zeitler, S. M.; Sun, P. B.; Reid, H. W.; Zakharov, L. N.; Golder, M. R.; Jasti, R. Controlled Polymerization of Norbornene Cycloparaphenylenes Expands Carbon Nanomaterials Design Space. *ACS Cent. Sci.* **2021**, *7*, 1056-1065. <https://doi.org/10.1021/acscentsci.1c00345>

11. Darzi, E. R.; Jasti, R. The Dynamic Size-Dependent Properties of [5]-[12] Cycloparaphenylenes. *Chem. Soc. Rev.* **2015**, *44*, 6401-6410. <https://doi.org/10.1039/C5CS00143A>
12. R. Jasti, J. Bhattacharjee, J. B. Neaton and C. R. Bertozzi, J. The Synthesis, Characterization, and Theory of [9]-, [12]-, and [18]Cycloparaphenylene: Carbon Nanohoop Structures. *Am. Chem. Soc.*, **2008**, *130*, 17646-17647. <https://doi.org/10.1021/ja807126u>
13. White, B. M.; Zhao, Y.; Kawashima, T. E.; Branchaud, B. P.; Pluth, M. D. Expanding the Chemical Space of Biocompatible Fluorophores: Nanohoops in Cells. *ACS Cent. Sci.* **2018**, *4*, 1173-1178. <https://doi.org/10.1021/acscentsci.8b00346>
14. Schaub, T. A.; Margraf, J. T.; Zakharov, L.; Reuter, K.; Jasti, R. Strain-promoted reactivity of alkyne-containing cycloparaphenylenes. *Angew. Chem. Int. Ed.* **2018**, *57*, 16348-16353. <https://doi.org/10.1002/anie.201808611>
15. Row, R. D.; Prescher, J. A. Cyclopropenethione-Phosphine Ligation for Rapid Biomolecule Labelling. *A. Org. Lett.* **2018**, *20*, 5614-5617. <https://doi.org/10.1021/acs.orglett.8b02296>